Forest Ecology and Management 613 (2026) 123776

Contents lists available at ScienceDirect

Forest Ecology and Management

journal homepage: www.elsevier.com/locate/foreco

SlashScan: An iOS application for real-time forest slash pile volume estimation and mapping

Heechan Jeong [a], Heesung Woo [a,*], Woodam Chung [a], Taejin Kim [a], Nathaniel Anderson [b]

[a] College of Forestry, Oregon State University, 1500 SW Jefferson Way, Corvallis, OR, United States
[b] Rocky Mountain Research Station, USDA Forest Service, Missoula, MT, United States

ARTICLE INFO

Keywords:
LiDAR
Mobile application
Smartphone sensor
3D mapping
Forest biomass
Forest management

ABSTRACT

Forest slash piles require effective management for site preparation and fire risk reduction. While pile burning remains a common disposal method, there is growing interest in utilizing these materials for energy and other bioproducts. Slash piles can serve as temporary carbon storage, and provide wildlife habitat, but they also contribute to surface fuel loads and increase site preparation costs if not properly utilized or disposed. Managing such low-value materials distributed across large forest landscapes poses logistical and economic challenges, especially when the volume and precise location are unknown. This study introduces SlashScan, a mobile application for iPhone and iPad that simultaneously estimates slash pile volume and generates location data in real time without additional equipment. The performance was validated by comparing volume estimates from 14 slash piles acquired using Unmanned Aerial Vehicle (UAV) based Light Detection and Ranging (LiDAR). The mean estimated volumes were 88.11 $m^3 \pm 33.51$ m^3 for UAV-LiDAR and 92.43 $m^3 \pm 39.18$ m^3 for SlashScan, with a mean difference of 4.31 m^3 . A paired t-test indicated no statistically significant difference between the two methods ($p > 0.05$). Strong agreement was further demonstrated by high coefficient of determination ($R^2 = 0.948$), low root mean square error (RMSE = 10.64 m^3), mean absolute error (MAE = 6.72 m^3), and mean absolute percentage error (MAPE = 6.76%). These results demonstrate that SlashScan provides volume estimates comparable to those from UAV-LiDAR while offering substantial advantages in portability, cost, and operational simplicity. This study offers a practical tool for improving forest slash management where accessibility and real-time data acquisition are essential.

1. Introduction

Slash piles are accumulations of forest residues such as branches and unmerchantable treetops that remain after logging or thinning operations. These residues, while often considered low-value or waste materials, may play multiple roles in post-harvest forest environments. They can act as temporary carbon storage, and provide wildlife habitat (Bojarski et al., 2023; Udali et al., 2025). However, when left unmanaged, accumulated residues contribute to surface fuel loads, and increase wildfire hazards (Grotta, 2019). Even when wildfire risk is not a concern, accumulations of slash can interfere with regeneration, replanting, and other forest management activities. To prevent fire risks, pile burning has been widely adopted as a common practice to dispose slash piles (Mott et al., 2021; Page-Dumroese et al., 2017). At the same time, because slash piles themselves are potential feedstocks for energy and bioproducts, interest has grown in their utilization as low-carbon alternatives within the forest bioeconomy (Nurek et al., 2019; Vanhala et al., 2013). It is already common practice in the forest industry to use slash and mill residues as fuel for the cogeneration of heat and power for primary manufacturing processes, including milling and drying. Nevertheless, the management of these dispersed and low-value materials across large forest landscapes involves inherent logistical and supply chain complexities. The efficient utilization or disposal of forest residues is hampered by uncertainties in their nature, quantity, and quality, making economic scaling difficult (Woo et al., 2019). Consequently, the effective management of slash piles has emerged as an essential role at the intersection of ecological concerns and economic viability, demanding better tools to inventory this resource.

In this context, accurate estimation of slash pile volume is fundamental to both disposal and utilization strategies. From a wildfire

* Correspondence to: College of Forestry, Oregon State University, 1500 SW Jefferson Way, Corvallis, OR 97331, United States.
E-mail address: heesung.woo@oregonstate.edu (H. Woo).

https://doi.org/10.1016/j.foreco.2026.123776
Received 10 February 2026; Received in revised form 30 March 2026; Accepted 31 March 2026
Available online 9 April 2026
0378-1127/© 2026 Published by Elsevier B.V.

management perspective, quantifying pile volume provides essential input for assessing total fuel loads, which inform fire behavior modeling and prescribed burning intensity (Barker et al., 2025; Hardy, 1996). From a utilization standpoint, reliable volume information supports biomass transportation logistics, cost estimation, and supply chain optimization for renewable energy production (Han et al., 2018; Han and Murphy, 2011). From an ecological standpoint, accurate estimation can guide the retention of some biomass on site to support various soil, habitat and biodiversity functions (Page-Dumroese et al., 2010; Riffell et al., 2011).

Traditionally, slash pile volume has been estimated using geometric approximations based on pile shape, an approach introduced in the 1980s and later incorporated into U.S. Forest Service guidelines (Hardy, 1996; Trofymow et al., 2014). These methods classify piles into idealized geometric forms, such as half-spheres, half-ellipsoids, paraboloids, and irregular solids, and compute volume using corresponding standard formulas based on measured dimensions including height, length, and width (Hardy, 1996). While these methods provided standardized protocols for management, they often failed to account for the irregular shapes and heterogeneous composition of piles, leading to significant inaccuracies (Long and Boston, 2014). For instance, Long and Boston (2014) found that geometric approximations showed substantially greater deviations from LiDAR-derived estimates than laser rangefinder measurements, with variability increasing for larger piles. Similarly, Zvěřina et al. (2025) found that manual measurements tended to overestimate pile volumes by around 35%. Moreover, larger piles tend to exhibit greater errors in volume estimation (Zvěřina et al., 2025).

Advances in LiDAR technology have significantly enhanced the precision of volume estimation for forest residues. For example, Trofymow et al. (2014) have demonstrated that LiDAR-based approaches outperform traditional geometric methods in estimating slash pile volumes in terms of both accuracy and reliability. In particular, UAV-mounted LiDAR systems have improved data acquisition efficiency, providing detailed measurements even in complex terrain and reducing fieldwork duration (Knyaz and Maksimov, 2014; Son et al., 2020; Trofymow et al., 2014). Despite these technical advantages, the operational application of UAV-LiDAR remains constrained by several factors. Although UAV-LiDAR systems provide high data precision, their practical use is constrained by high equipment costs and time-consuming calibration and processing steps (Bartmiński et al., 2023; Spiers et al., 2025). These factors limit real-time applicability and workflow standardization required for the efficient, large-scale inventory of low-value material like forest residues. Furthermore, such technologies often require specialized training that many forestry field staff do not have. These economic and operational constraints have limited the routine use of UAV-LiDAR in forest management applications that demand timely decision-making and field portability (Dandois and Ellis, 2013; Moe et al., 2020). Consequently, there is an increasing need for cost-effective, lightweight, and real-time alternatives capable of delivering comparable accuracy for on-site volume assessment.

Given these operational constraints, two principal low-cost alternatives have emerged for field-based 3D reconstruction: Structure-from-Motion (SfM) photogrammetry and mobile LiDAR. SfM reconstructs three-dimensional surfaces from overlapping photographs and has been applied across a range of environmental measurement tasks (Iglhaut et al., 2019). However, it typically requires longer post-processing time and is sensitive to ambient lighting conditions, and wind-induced movement of vegetation (Iglhaut et al., 2019; McNicol et al., 2021), factors that are frequently encountered in operational forestry settings. In contrast, LiDAR employs active laser scanning that operates independently of these environmental factors (Lim et al., 2003), making it inherently more suitable for real-time field applications. The rapid advancement of mobile sensing technologies has made LiDAR-based 3D acquisition increasingly accessible. Modern smartphones and tablets are now equipped with Global Navigation Satellite System (GNSS) receivers, Inertial Measurement Units (IMU), and depth cameras, enabling numerous applications in environmental monitoring, mapping, and forest measurement (Oikawa et al., 2025; Tatsumi et al., 2023). The integration of LiDAR sensors into iOS devices in 2020 further expanded these capabilities, offering a practical platform for cost-effective and real-time three-dimensional data acquisition without the need for specialized equipment or training. Several studies have demonstrated the potential of iOS-based LiDAR for forest inventory applications such as stem mapping and diameter-at-breast-height (DBH) estimation (Castel et al., 2022; Gollob et al., 2021; Guenther et al., 2024). However, these studies have primarily addressed structured and relatively uniform forest conditions. In contrast, slash piles often exhibit complex and irregular geometries with large and uneven volumes, which can make accurate scanning and surface reconstruction more challenging. Consequently, existing mobile LiDAR approaches cannot be directly applied to complex pile structures. Although mobile LiDAR offers clear practical advantages in terms of cost and portability, its capability for accurate slash-pile volume estimation has not yet been systematically evaluated.

To address these limitations, the integration of advanced spatial mapping and surface-modeling algorithms is required. Among these, Real-Time Appearance-Based Mapping (RTAB-Map) provides a robust simultaneous localization and mapping (SLAM) framework that stabilizes 3D reconstruction by mitigating drift and registration errors in dynamic or complex outdoor environments (Labbé and Michaud, 2011; Labbé and Michaud, 2013; Labbé and Michaud, 2018, 2019). In parallel, Poisson Surface Reconstruction (PSR) with a Neumann Boundary Condition (NBC) generates watertight, continuous mesh surfaces that more accurately represent complex, irregular geometries than conventional triangulation-based methods (Kazhdan et al., 2006; Kazhdan and Hoppe, 2013). The integration of these complementary algorithms provides the foundation for developing lightweight and field-deployable tools capable of accurate 3D reconstruction using mobile LiDAR.

Building upon this framework, this study introduces SlashScan, an iOS-based mobile application developed for real-time slash-pile volume estimation and on-site 3D mapping. The system integrates RTAB-Map-based spatial stabilization with PSR-NBC surface modeling to perform volumetric reconstruction entirely on-device. While building on established 3D reconstruction workflows used in terrestrial laser scanning (TLS) and mobile laser scanning (MLS), SlashScan uniquely enables their integration into a fully self-contained mobile platform that supports real-time, on-device volume estimation without external processing, specialized hardware, or trained operators. This combination of field portability, low cost, and immediate output addresses key operational barriers that have limited the routine adoption of 3D scanning for slash pile inventory. The performance of SlashScan was evaluated against UAV-LiDAR benchmarks, which serve as reference data for high-precision volume estimation. The results suggest that mobile LiDAR-based solutions can function as accessible and economically viable alternatives for operational slash management, supporting wildfire mitigation and biomass utilization efforts.

2. Materials and methods

2.1. Overall research workflow

The overall research workflow of this study consists of three main phases as shown in Fig. 1. Phase 1 (App development) focuses on building the internal data-processing pipeline of SlashScan. In this phase, raw LiDAR sensor data are transformed into structured 3D models through a sequence of modules, including point-cloud mapping, surface reconstruction, hole filling, and mesh cropping. The processed 3D mesh is then stored with GNSS tagging, and the final volume estimation is performed directly within the mobile application. Phase 2 (Field test) involves two parallel measurement workflows: SlashScan and UAV-LiDAR workflow. The SlashScan workflow comprises on-site data collection, in-app mapping and processing, and automated volume

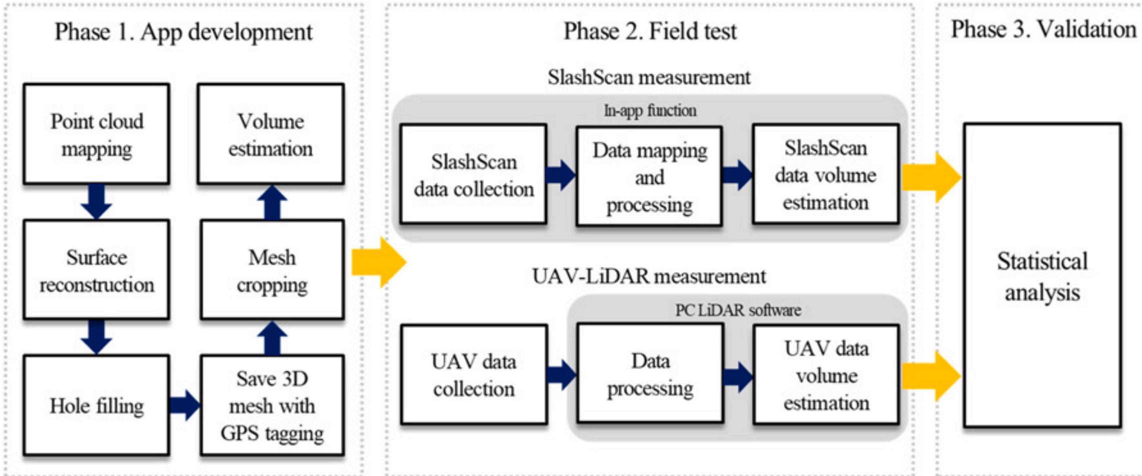

Fig. 1. Diagram with the overall research process.

estimation. The UAV-LiDAR workflow includes aerial data acquisition, data processing using PC-based LiDAR software, and corresponding volume estimation. These parallel datasets allow for a direct comparison of measurement performance under consistent field conditions. Phase 3 (Validation) evaluates the accuracy and reliability of SlashScan-derived volume estimates. The SlashScan and UAV-LiDAR datasets are statistically compared using a paired *t*-test to examine whether significant differences exist between the two measurement approaches, thereby assessing the overall performance of the proposed mobile LiDAR system.

2.2. Study site description

This study was conducted in a representative Douglas-fir (*Pseudotsuga menziesii*) stand located within Starker Forest (44°36'20"N, 123°20'52"W) in OR, United States, which is managed by Starker Forests Inc. The location and map of the study site are shown in Fig. 2, and a representative field photograph of a slash pile is presented in Fig. 3. The study site consists of a clear-cut area covering approximately 13.0 ha. The elevation was 266 m above sea level, and the slope ranged from 0% to 20%. The logging operation was conducted using a cut-to-length (CTL) harvesting system, in which individual trees were processed into logs measuring 10.97 m (36 feet) in length, on average, based on processor data. Harvested volume from naturally regenerated stands was dominated by Douglas-fir (81.99%), followed by Grand fir (*Abies grandis*, 17.95%) and Bigleaf maple (*Acer macrophyllum*, 0.06%). All slash remaining after harvesting was piled by machines.

2.3. SlashScan development

The SlashScan application was developed on a 13-inch MacBook Pro using the Xcode 16 development environment. Swift 5 was adopted for front-end development, which includes the user interface and app control, while C++ was used for the back-end processing of LiDAR data. To enable data processing and 3D reconstruction from iOS LiDAR input,

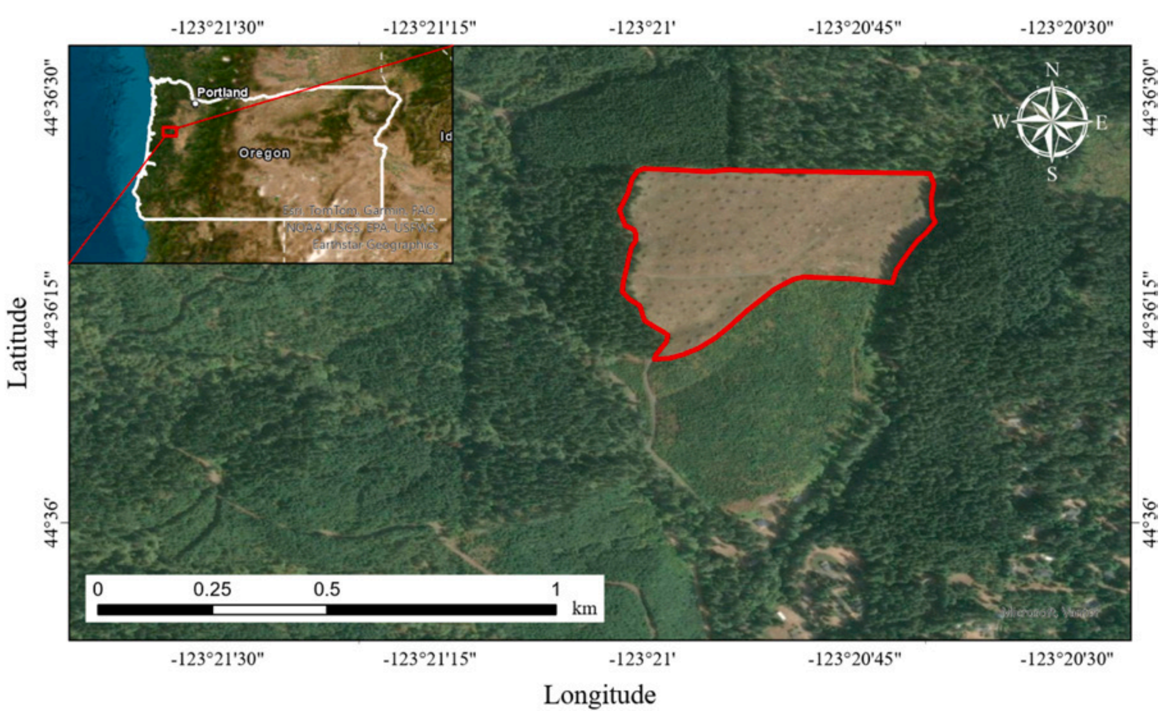

Fig. 2. Case study area located in Starker Forest, OR, United States.

Fig. 3. Field photograph of a slash pile on the research site.

several open-source C+ + libraries were integrated, including OpenCV, Point Cloud Library (PCL), Eigen, the Visualization Toolkit (VTK), OpenGL, and Real-Time Appearance-Based Mapping (RTAB-Map). To enable slash pile coordinate mapping, the application adopted Apple Maps, which is natively supported on iOS, to ensure usability in forest environments with limited internet connectivity.

2.3.1. Point cloud mapping

Based on the data acquired from the device, high-precision 3D point cloud mapping was performed using the RTAB-Map algorithm. RTAB-Map employs LiDAR data to perform SLAM, incorporating loop closure detection to minimize drift errors and enhance the overall consistency of the mapped environment (Labbé and Michaud, 2011; Labbé and Michaud, 2013; Labbé and Michaud, 2018, 2019). The algorithm operates by creating a graph where nodes represent the device's pose at a given time, and edges represent the spatial constraints between poses. A key feature of RTAB-Map is its appearance-based loop closure detection mechanism. When the device revisits a previously mapped area, the algorithm identifies this loop by comparing the current visual information against a database of past views using a bag-of-words approach. The probability of a loop closure is updated using a Bayesian filter:

$$P(L_t|Z_{1:t}) \propto P(Z_t|L_t)\sum_{L_{t-1}} P(L_t|L_{t-1})P(L_{t-1}|Z_{1:t-1})$$

where $P(L_t|Z_{1:t})$ is the posterior probability of the device being at location L_t given all observations $Z_{1:t}$ up to time t, $P(Z_t|L_t)$ represents the likelihood of observing Z_t at location L_t, and $P(L_t|L_{t-1})$ is the transition probability between consecutive locations. Upon successful loop closure detection, a graph optimization process is triggered to minimize the accumulated odometry drift. This optimization is formulated as a non-linear least-squares problem:

$$\underset{X}{\mathrm{argmin}}\sum_{i,j} e\left(x_i, x_j, z_{ij}\right)^T \Omega_{ij} e\left(x_i, x_j, z_{ij}\right)$$

where $e\left(x_i, x_j, z_{ij}\right)$ represents the error between the predicted and measured relative poses, and Ω_{ij} is the information matrix representing the uncertainty of the measurement. Following the mapping process, the generated point cloud was subsampled using a fixed spatial interval of 2 cm to reduce computational overhead during subsequent processing and visualization steps while maintaining sufficient detail for accurate reconstruction.

2.3.2. Surface reconstruction

Slash piles exhibit highly complex structures due to the irregular mixture of materials and variable shapes they comprise (Long and Boston, 2014). To address these challenges, this study employed the PSR implemented through the C+ + based open-source Point Cloud Library (Kazhdan et al., 2006; Rusu and Cousins, 2011). This method is characterized by its ability to generate smooth, continuous, and topologically consistent surfaces by solving the Poisson equation (Vizzo et al., 2021). The core principle of the PSR involves finding a scalar indicator function χ that distinguishes between the interior and exterior of the object. The gradient of this function, $\nabla\chi$, is non-zero only at the surface and corresponds to the surface normals. The oriented points from the point cloud provide a vector field V that approximates this gradient. By applying the divergence operator to both fields, we arrive at the Poisson equation:

$$\nabla^2\chi = \nabla\cdot V$$

where ∇^2 is the Laplacian operator. Solving this partial differential equation for χ yields a continuous scalar field from which the final surface is extracted as an isosurface. The reconstructed mesh was generated by treating each point in the point cloud as a vertex and connecting these vertices into triangles to form a 3D geometric surface. Each triangular face was assigned a color based on RGB information captured by iOS ARKit.

2.3.3. Mesh hole filling

Because it is impossible to capture every part of a scanned surface, the reconstructed models typically contain holes caused by various factors (Brunton et al., 2009). To preserve surface smoothness and avoid abrupt transitions at mesh boundaries such as sharp edges or tearing, the PSR was performed incorporating the NBC (Kazhdan and Hoppe, 2013). The NBC specifies the normal direction (gradient) along mesh boundaries, thus enabling the generation of smooth and watertight surfaces even in regions with incomplete or sparse data. The NBC is mathematically expressed as:

$$\frac{\partial\chi}{\partial n} = 0$$

where n is the normal to the boundary. This boundary condition ensures that the surface smoothly extends over areas with missing data, effectively filling holes without creating artificial seams or discontinuities.

2.3.4. Save 3D mesh with GPS tagging

The processed mesh data is stored within the SlashScan application on the iOS device, along with the corresponding latitude, longitude, and altitude information acquired during data collection. The stored coordinates represent the last recorded geolocation of the device at the time of data acquisition. Each recorded data entry is integrated with Apple Maps through the iOS MapKit framework, enabling users to visualize the pile's location directly on the map interface. In cases where GNSS signals are weak or unavailable, resulting in the absence of geolocation data, the mesh is saved without spatial coordinates. However, the application is designed to allow users to manually assign or edit the geolocation information at a later stage within the app interface, ensuring flexibility in various field conditions.

2.3.5. Mesh cropping

The reconstructed 3D mesh may contain not only the target slash pile but also extraneous objects. For example, large rocks or soil and debris piles may be close to slash piles on log landings, which are often cleared and flattened by heavy equipment. Inclusion of such objects occurs because the iOS LiDAR sensor captures all elements within its maximum sensing range of 5 m, resulting in the mapping of surrounding environments along with the slash pile. A conventional approach to addressing this issue involves using a predefined 3D cropping box to trim the data. To address this problem, SlashScan allows users to manually delineate the pile area by drawing a polygon directly on the device screen via touch interaction. The system then applies an OpenGL-based inverse projection and view transformation to map the 2D polygon onto the 3D mesh. Mesh components outside the delineated area are excluded, leaving only the targeted pile for subsequent volume estimation.

2.3.6. Volume estimation

The volume of each slash pile was calculated using the tetrahedral summation method (TSM), a widely adopted technique for three-dimensional volume estimation known for its high accuracy (Lin et al., 2024). TSM computes the total volume by summing the signed volumes of tetrahedra formed between each triangular face of the reconstructed mesh and a reference origin point (Zhang and Chen, 2001) as illustrated in Fig. 4(a). The volume can be computed by summing the volumes of tetrahedrons:

$$V = \frac{1}{6}\sum_{k} |(a_k - O)\cdot[(b_k - O) \times (c_k - O)]|$$

where the sum is over all N triangles in the mesh, a_k, b_k, c_k are the vertices of the k-th triangle, and the origin point O. To perform this calculation, the surface normal vector of each triangle must first be determined, which is obtained by computing the cross product of two edge vectors of the triangle. The reconstructed mesh forms a closed surface representing the slash pile as shown in Fig. 4(b). Since slash piles are not always formed on flat ground and are often located on sloped terrain (Gotou and Nishimura, 2002), it is critical to incorporate ground topography into the volume computation. In this study, the ground plane was defined based on the mean coordinates of the user-selected polygon during the cropping process. This average ground level served as the origin for forming tetrahedra with each triangular face in the mesh. By referencing the actual mean ground elevation, the method accounts for terrain inclination and mitigates errors that would arise from assuming a flat ground surface.

2.4. Field measurement

The field measurement process involved data acquisition and volume estimation using two platforms: a UAV-mounted LiDAR system and the SlashScan application installed on an iOS device. Accurate quantification of slash pile volume is often limited by the simplifying assumptions required in conventional geometric measurements, particularly for irregularly shaped piles. Previous comparative studies have shown that LiDAR-based techniques yield more reliable volume estimates by capturing the actual three-dimensional structure of residue piles. Long and Boston (2014) demonstrated that the laser rangefinder produced results that were closer to the LiDAR-generated estimates in more than two-thirds of the samples, whereas the geometric measurements varied more from LiDAR estimates, concluding that LiDAR-derived measurements most accurately represented the true pile geometry. Similarly, Casey (2015) reported that the TLS LiDAR achieved concordance correlation coefficients of approximately 0.9 compared to a commercial laser rangefinder, indicating that LiDAR-based systems can achieve accuracy comparable to established reference methods. Accordingly, LiDAR sensing was adopted in this study for both aerial and ground-level measurements to ensure accurate volumetric representation of slash piles.

The UAV-based system was used to acquire aerial LiDAR data for volumetric analysis, while the SlashScan application enabled ground-level 3D data acquisition and in-app volume estimation using the device's built-in LiDAR sensor. The UAV LiDAR system consisted of a LiAir V70 unit (GreenValley International, Berkeley, CA, USA) mounted on a Matrice 300 RTK (DJI, Shenzhen, China), enabling aerial point cloud collection. Ground-based data acquisition was conducted using an Apple iPad Pro 13-inch (Apple, Cupertino, CA, USA) equipped with an

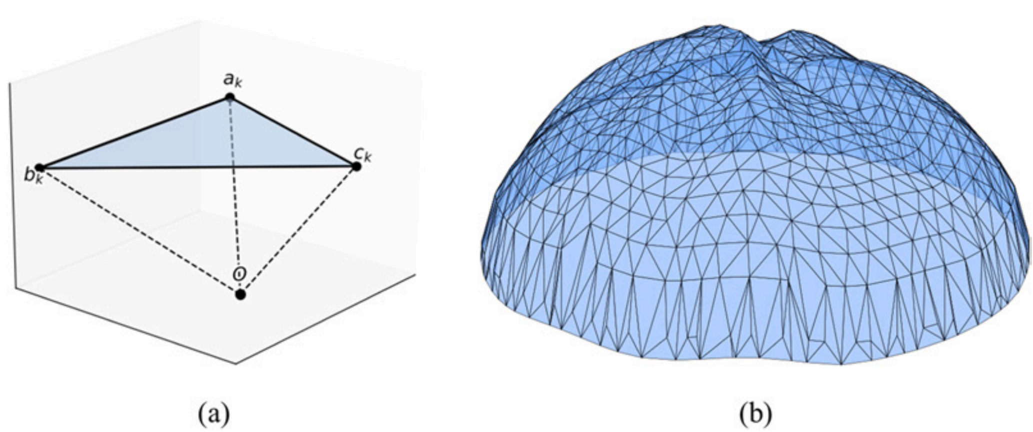

Fig. 4. TSM for slash-pile volume estimation. (a) For each triangular face ($\boldsymbol{a_k}, \boldsymbol{b_k}, \boldsymbol{c_k}$) of the reconstructed surface, a tetrahedron is formed with the origin $\boldsymbol{O}$; the total volume is obtained by summing the signed volumes of all such tetrahedra. (b) Example of a triangulated surface (pile-shaped mesh) used for the computation.

integrated LiDAR sensor. Detailed specifications of all devices and system configurations are provided in Fig. 5.

2.4.1. UAV LiDAR measurement

Flight path planning was conducted using UgCS software (SPH Engineering, Baloži, Latvia), which enables real-time communication between the drone and the remote controller. To maintain consistent LiDAR coverage across the survey area, a terrain-following was implemented, maintaining an altitude of 50 m above ground level. This approach allowed the UAV to ascend or descend as needed in response to terrain variation. The reference surface for terrain following was defined using the Shuttle Radar Topography Mission (SRTM) 1 Arc-Second Global Digital Elevation Model (DEM), provided by the United States Geological Survey (USGS), which offers a spatial resolution of 30 m. The UAV was programmed to fly at a speed of 5 m/s with a side overlap of 50%, following a mission path consisting of 15 flight strips. UAV LiDAR data acquisition was performed along this predefined path. The effective flight duration was approximately 17 min, excluding takeoff, landing, and calibration time. Simultaneously, seven ground control points were recorded at each site using the Trion V1 GNSS Receiver (FJDynamics, Singapore), which provided geodetically corrected coordinates. These control points were used to georeference the point cloud data and ensure precise spatial alignment during post-processing.

The point cloud data acquired from the UAV-LiDAR system were initially georeferenced using LiGeoReference (GreenValley International, Berkeley, CA, USA), and further processed using LiDAR360 version 5.4 (GreenValley International, Berkeley, CA, USA). Given the relatively lower spatial resolution of UAV acquired point clouds compared to ground-based LiDAR data, a volumetric estimation was performed by aggregating the point cloud data into a grid with a spatial resolution of 10 cm. The total volume of each slash pile was then calculated by summing the volume elements within the defined grid.

2.4.2. SlashScan measurement

Ground-based scanning of 14 slash piles corresponding to UAV-LiDAR data was conducted using SlashScan application. The scans were performed utilizing a built-in LiDAR sensor integrated with the Apple iPad 13-inch Pro. Upon pressing the scanning button within the app, loop closure and SLAM processes were automatically initiated through the embedded RTAB-Map algorithm.

To comprehensively capture the geometric structure of each pile, data acquisition was performed by slowly circling each pile at an approximate distance of 2 m from the pile surface, as illustrated in Fig. 6. Although the nominal maximum range of the iOS LiDAR sensor is about 5 m, measurement accuracy decreases beyond 2 m because of signal attenuation and depth uncertainty (Tondo et al., 2023). Each scan was conducted in a continuous 360-degree motion around the pile, covering both horizontal and vertical perspectives. To obtain a dense and homogeneous point cloud, the scanning movement was kept at a speed below approximately 1 m/s.

When a pile's height exceeded the operator's reach, the upward viewing angle of the iOS LiDAR sensor limited coverage of the upper surface. In such cases, the unscanned upper region was reconstructed through the NBC-based surface interpolation described in Section 2.3.3, producing a watertight mesh that maintained geometric continuity with the directly scanned portion, as shown in Fig. 7. After scanning, the SlashScan application automatically processed the acquired point cloud through the processing pipeline described in Fig. 1. The processed data were stored individually for each slash pile.

2.5. Validation of SlashScan volume estimation

The validation framework was structured as a two-stage comparative analysis between SlashScan and UAV-LiDAR, with the UAV-LiDAR-derived estimates serving as the reference standard throughout. For each of the 14 slash piles, three geometric quantities were extracted from both the SlashScan and UAV-LiDAR datasets: pile maximum height, 2D projected area, and volume. Pile maximum height was defined as the maximum normal distance from the ground plane fitted to the polygon boundary to the highest point of the mesh. The 2D projected area was defined as the ground-level polygon footprint area.

The first stage evaluated the agreement between the two platforms for pile maximum height and 2D projected area using RMSE, MAPE, and the coefficient of determination (R^2). To further isolate the contribution of the reconstructed 3D surface profile to volumetric discrepancy, a dimensionless shape factor k was computed for each pile:

$$k = V / (H \times A)$$

where V is the estimated volume, H is the pile maximum height, and A is the 2D projected area. This shape factor represents the fullness of the 3D pile profile relative to the bounding prism defined by H and A; a value of $k = 1$ would indicate a perfectly rectangular prism, while lower values reflect tapered or irregular geometries. Since volume is the product of height, area, and shape factor, the relative volume difference ($\Delta V/V$) can be approximated as the sum of the relative differences in height ($\Delta H/H$), area ($\Delta A/A$), and shape factor ($\Delta k/k$), following a first-order multipli-

Matrice 300 RTK	Specifications
Full Width	0.67m
Full Length	0.81m
Full Height	0.43m
Payload Capacity	2.7kg
Max. Flight Time	55minutes
Max. Flight Speed	23m/s

(a)

LiAir V70	Specifications
LiDAR	Livox AVIA
Scan Rate	240,000pts/s
Field of View	70.4° x 4.5°
Return	Triple
Detection Range	320m

(b)

iPad Pro M4	Specifications
Chip	Apple M4 chip
CPU Core	9-Core
GPU Core	10-Core
Memory	8GB
LiDAR Range	5m
Camera	12MP Wide

(c)

Fig. 5. Specifications of (a) Matrice 300 RTK UAV, (b) LiAir V70 UAV LiDAR, (c) and iPad Pro 13-inch M4.

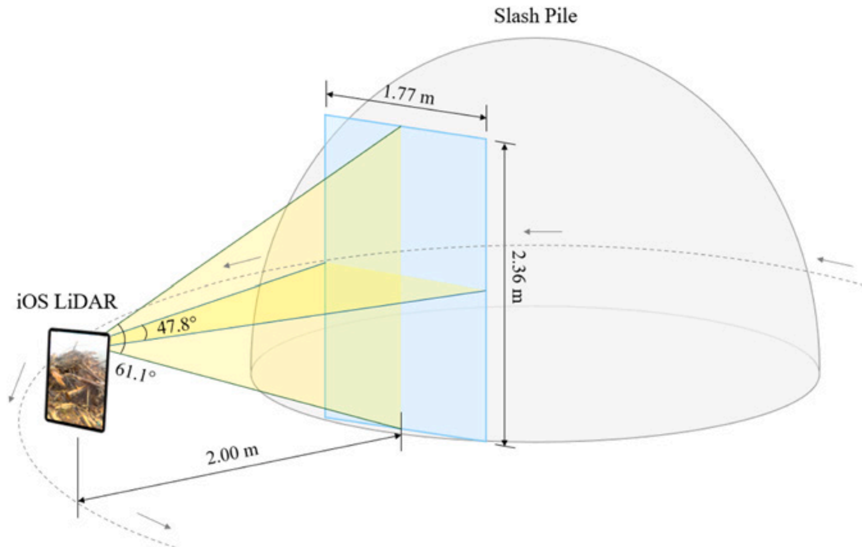

Fig. 6. Individual pile 360-degree scanning using SlashScan app with iPad 13-inch Pro.

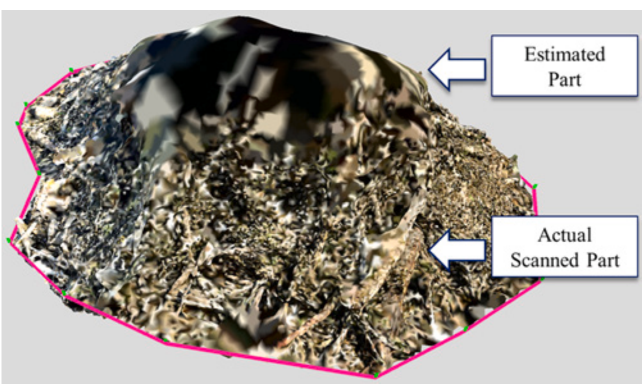

Fig. 7. Visualization of a reconstructed slash pile showing the actual scanned region and the interpolated upper surface generated during mesh reconstruction.

cative error propagation framework. This decomposition made it possible to attribute the volumetric discrepancy for each pile to its dominant source, and to distinguish errors in basic geometric measurement from errors in the reconstructed surface morphology.

The second stage assessed overall volume accuracy through direct comparison of SlashScan and UAV-LiDAR volume estimates. A paired *t*-test was conducted to determine whether a statistically significant difference existed between the mean volumes of the two methods, with the significance level set at $\alpha = 0.05$. The mean difference, its 95% confidence interval, and the corresponding t-statistic, degrees of freedom, and p-value were reported. Complementary accuracy metrics including RMSE, MAE, and MAPE were also computed. For visual assessment of agreement, a scatter plot was constructed incorporating a 1:1 reference line, a $\pm$ 10% agreement band, and fitted regression lines for all data and excluding the largest-error case. All statistical analyses were performed using Python 3.10 with the SciPy and NumPy libraries.

3. Results and discussion

3.1. SlashScan system overview and functionality

SlashScan was developed as an iOS-based mobile application that integrates LiDAR scanning, three-dimensional (3D) reconstruction, volumetric analysis, and geospatial mapping within a single platform. The application is available for download from the Apple App Store (https://apps.apple.com/us/app/slashscan/id6740838119) and operates entirely on-device, eliminating the need for external computation or internet connectivity during field use.

The principal interfaces and components of the application are illustrated in Fig. 8. A user guide assists users through data collection and management, followed by a structured project folder system that enables efficient organization of multiple scans. Each dataset is automatically saved with preview images and timestamps, allowing users to review and compare previous measurements. The reconstructed pile is visualized as a textured 3D mesh, and a polygon-based cropping tool is provided for defining pile boundaries and computing pile volumes directly within the app. While this manual boundary definition allows flexibility in irregular field conditions, it may introduce operator-dependent variation; thus, automated boundary detection and guided snapping algorithms are being considered for future versions to enhance consistency across different operators. Each scan is geotagged using the device's built-in GNSS module and displayed on an interactive map, enabling spatial referencing and site-level coordination. An offline map function further supports operation in remote forest areas without network connectivity. The integrated structure of the application allows for LiDAR-based measurement, visualization, and georeferenced data management within a mobile environment suitable for field-based forestry operations.

3.2. Slash pile measurement and validation results

The volume of the 14 slash piles was estimated using both the developed SlashScan application and a UAV-LiDAR system, which served as the benchmark for this study. Despite the inherent variability across pile sizes, all SlashScan on-device data processing following scan completion, including point-cloud reconstruction, surface meshing, and volumetric computation, was completed within approximately 30 s per pile. This near-real-time processing capability highlights the efficiency of the mobile LiDAR workflow compared to conventional UAV-based methods that require separate post-processing on external hardware.

A total of 14 paired datasets were constructed by matching each slash pile scanned by SlashScan with its corresponding UAV-LiDAR dataset, as shown in Fig. 9. These paired datasets served as the basis for evaluating measurement consistency between the aerial and ground-based LiDAR platforms. The structural metrics and volume estimates obtained from both methods are summarized in Table 1, and the pile IDs correspond to the numeric labels displayed in Fig. 9. Across all piles, mean pile

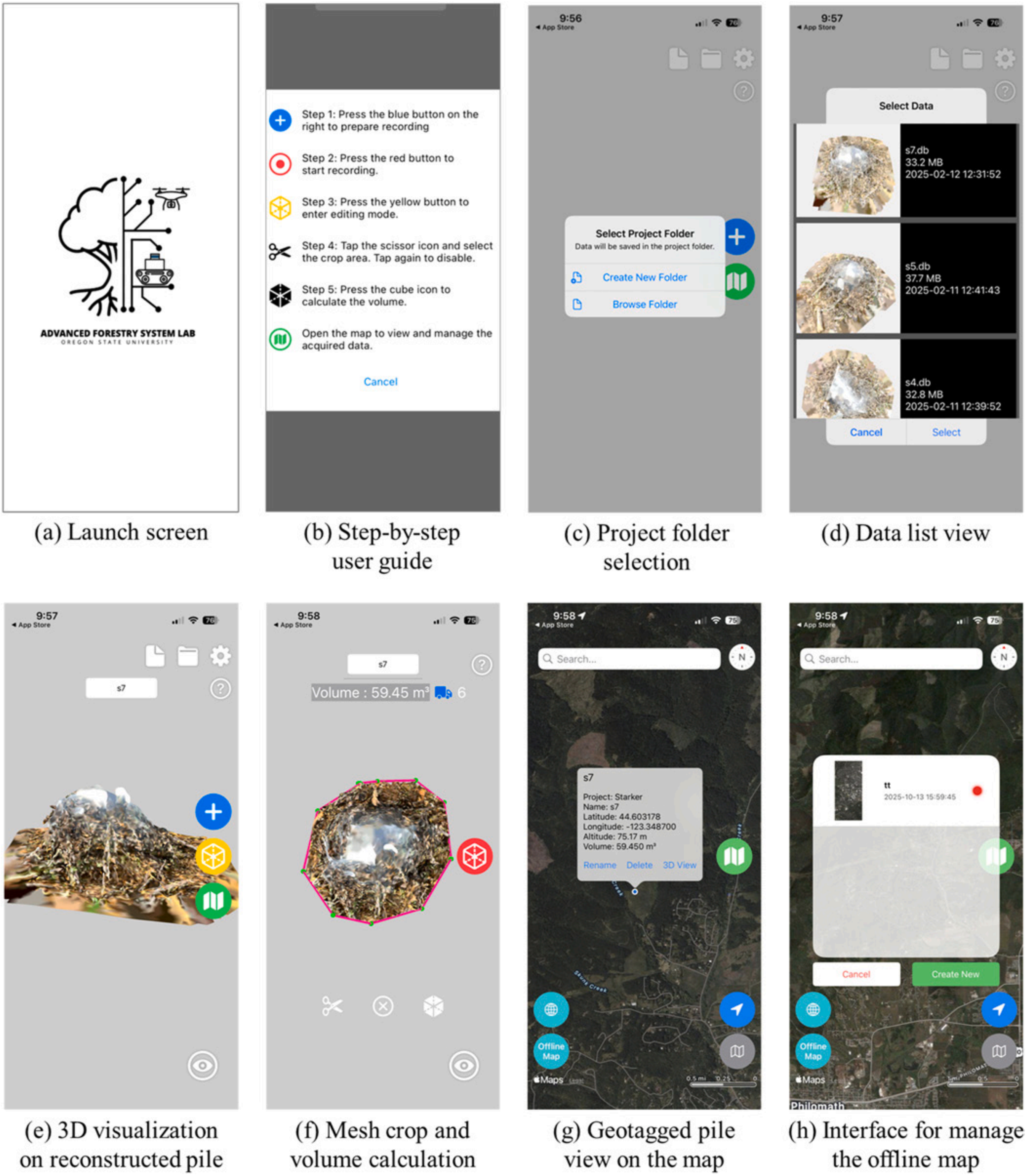

Fig. 8. Screenshots of the SlashScan application.

maximum height was 3.03 m for SlashScan and 3.11 m for UAV-LiDAR, and mean 2D projected area was 65.88 m^2 and 64.32 m^2, respectively. Mean volume estimated by UAV-LiDAR was 88.11 m^3 (SD = 33.51 m^3), while SlashScan produced a mean of 92.43 m^3 (SD = 39.18 m^3). The coefficient of variation (CV) was 38.03% for UAV-LiDAR and 42.39% for SlashScan, indicating slightly greater relative variability in the iOS LiDAR estimates. Overall, the mean volume difference between the two methods was 4.31 m^3, corresponding to 4.89% of the UAV-LiDAR mean.

3.2.1. Component metrics

Prior to direct volume comparison, agreement between SlashScan and UAV-LiDAR was evaluated for two intermediate geometric quantities: pile maximum height and 2D projected area, as shown in Fig. 10. For pile maximum height, SlashScan produced a mean of 3.03 m

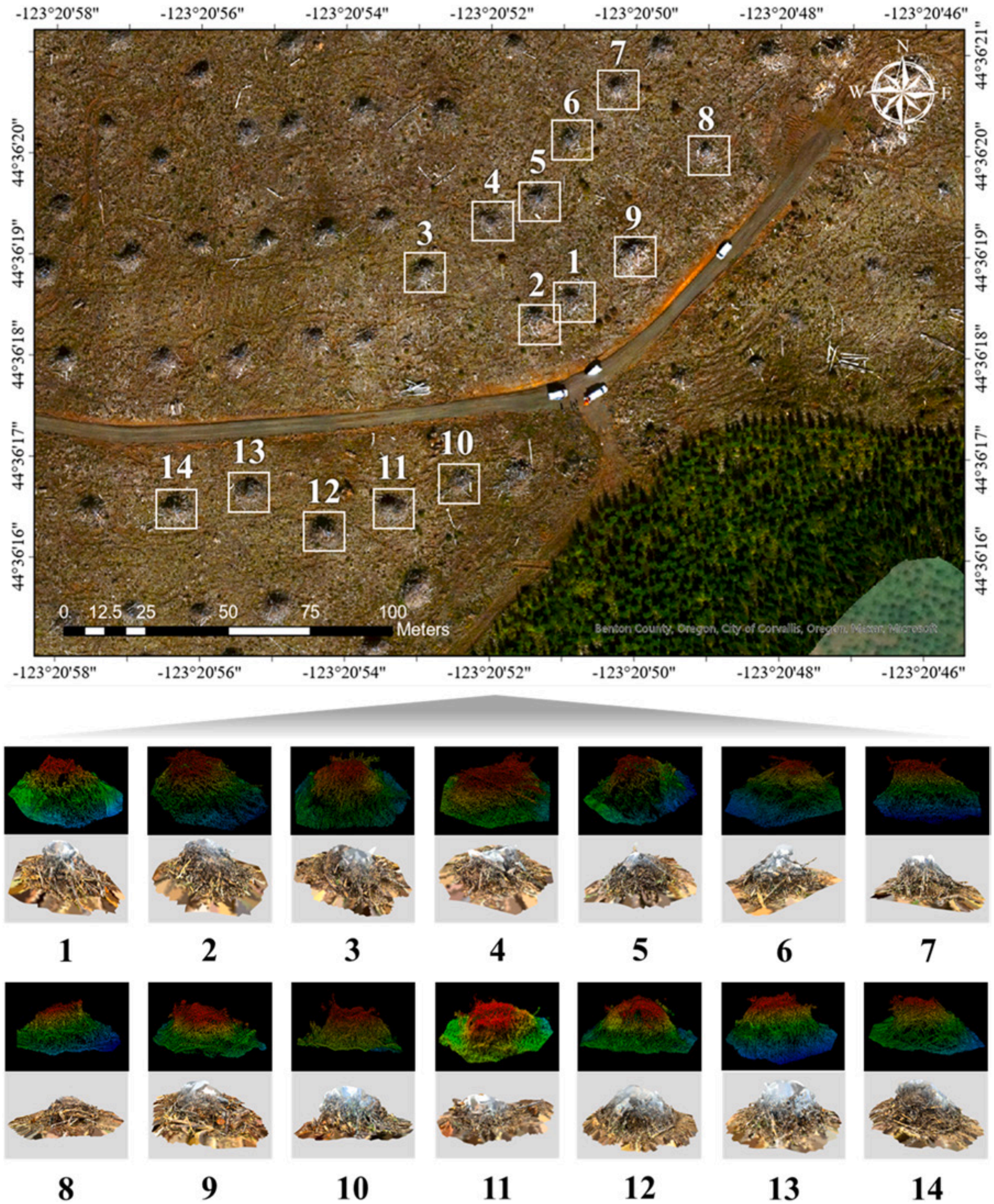

Fig. 9. Spatial distribution and corresponding 3D representations of the 14 paired datasets used for validation. The upper orthomosaic shows the locations of 14 individual slash piles within the study site. The lower panels present paired 3D models of the same piles, with the upper rows showing point-cloud reconstructions derived from UAV-LiDAR data and the lower rows displaying textured mesh models generated from the SlashScan application.

compared to 3.11 m from UAV-LiDAR, yielding a mean difference of −0.08 m (-2.6% relative to the UAV-LiDAR mean). The RMSE for height was 0.18 m and the MAPE was 4.5%, with $R^2 = 0.887$ (Fig. 10a). UAV-LiDAR tended to produce slightly higher values for most piles, which is consistent with the top-down viewing geometry of the aerial platform capturing the true apex of the pile more completely than the ground-based sensor. This discrepancy was more pronounced for taller piles: among piles with UAV-LiDAR heights exceeding the median (3.17 m), SlashScan measured height 5.2% lower on average, compared to 0.8% higher for shorter piles, where individual values varied in both directions. This pattern is consistent with the limited upward viewing angle and 5 m sensing range of the iOS LiDAR, which increasingly restricts coverage of the upper surface as pile height approaches or exceeds the operator's eye level. For 2D projected area, SlashScan yielded a mean of 65.88 m^2 versus 64.32 m^2 from UAV-LiDAR, corresponding to a mean difference of 1.56 m^2, or 2.4% relative to the UAV-LiDAR mean. The RMSE for 2D projected area was 3.48 m^2, the MAPE = 4.7%, and $R^2 = 0.964$ (Fig. 10b). Because the pile boundary is manually delineated by the operator on both platforms, the observed area differences reflect polygon placement variability rather than a systematic sensor-level bias.

Table 1
Structural metrics and volume estimates for all piles measured by SlashScan and UAV-LiDAR.

Validation						
Pile ID	SlashScan			UAV-LiDAR		
	Max. Height (m)	Projected Area (m^2)	Volume (m^3)	Max. Height (m)	Projected Area (m^2)	Volume (m^3)
1	2.79	58.83	66.66	2.88	58.86	68.23
2	2.68	60.12	70.53	2.72	56.35	67.96
3	3.52	49.10	73.04	3.61	47.93	75.51
4	2.43	52.91	61.81	2.57	46.52	56.61
5	2.57	60.25	61.21	2.45	56.34	60.88
6	3.46	51.44	73.48	3.12	48.34	71.50
7	3.00	47.13	62.58	3.01	48.31	60.29
8	2.13	47.17	38.17	2.13	47.30	41.02
9	3.14	95.22	98.01	3.52	91.90	107.96
10	3.06	88.88	157.06	3.22	91.15	123.10
11	3.05	74.61	100.15	3.31	80.48	93.01
12	3.41	69.69	135.08	3.59	66.26	125.58
13	3.72	80.68	152.83	3.83	79.14	141.85
14	3.43	86.27	143.34	3.52	81.53	140.09
Mean	3.03	65.88	92.43	3.11	64.32	88.11

3.2.2. *Shape factor analysis*

To determine whether the observed volumetric discrepancies were attributable to errors in the component metrics or to differences in the reconstructed 3D surface profile, a shape factor was computed for each pile. The mean shape factor was 0.449 for SlashScan and 0.434 for UAV-LiDAR, indicating that SlashScan reconstructions tended to produce slightly fuller pile profiles. Shape factor variability was also greater for SlashScan, with a CV of 15.5% compared with 12.1% for UAV-LiDAR, reflecting the higher sensitivity of the ground-based reconstruction to pile morphology.

Using the first-order decomposition framework described in Section 2.5, the relative volume difference for each pile was separated into contributions from height, area, and shape factor. Across most piles, no single component dominated the volumetric error; the three contributions varied in direction depending on pile-specific geometry (Fig. 11). However, Pile 10, which exhibited the largest volume overestimation (27.6%), illustrates a case where the shape factor component was clearly dominant. For this pile, SlashScan measured height 5.0% lower and area 2.5% smaller than UAV-LiDAR, yet produced a shape factor 37.7% higher (Fig. 11). The positive shape factor deviation more than compensated for the negative maximum height and projected area, driving the overall overestimation. Representative examples of this reconstruction difference are presented in Fig. 12: whereas the convex-top pile (Pile 1; Fig. 12a-c) shows high geometric consistency between the two platforms, the concave-top pile (Pile 10; Fig. 12d-f) reveals that the UAV-LiDAR captured a concave depression on the upper surface while the SlashScan reconstruction interpolated this region as a convex form. A similar but less pronounced pattern was observed for Pile 11, where SlashScan overestimated volume by 7.7%. For this pile, height was 7.9% lower and area was 7.3% smaller in SlashScan, but the shape factor was 26.0% higher, more than compensating for the lower geometric dimensions.

Across all piles, a directional trend was also observed between pile height and shape factor discrepancy. Among taller piles (UAV-LiDAR pile maximum height $\geq$ 3.17 m), the mean shape factor difference was 10.6%, whereas shorter piles showed a mean difference of −3.2%. This pattern suggests that as pile height increases, the proportion of upper surface not directly scanned by the ground-based sensor also increases, leading to greater reliance on surface interpolation and a systematic positive bias in reconstructed fullness. Excluding Pile 10, the remaining 13 piles showed a mean volume difference of 1.8%, with mean shape factor differences of 1.1%, indicating generally good agreement in both component geometry and reconstructed surface form.

3.2.3. *Volume estimation accuracy*

The paired *t*-test results for all 14 slash piles are presented in Table 2. The test yielded a p-value of 0.134, which is substantially greater than the significance threshold of $\alpha = 0.05$, failing to reject the null hypothesis that the mean volumes estimated by the two methods are equal. The t-statistic was 1.60 with 13 ° of freedom, and the 95% confidence interval for the mean difference ranged from -1.52 m^3 to 10.14 m^3, encompassing zero.

While the *t*-test supports the conclusion that the means are not statistically different, it does not capture the magnitude of individual estimation errors. To provide a more comprehensive assessment, several error metrics were computed from the paired dataset. When evaluated across all 14 paired samples, the overall error levels were relatively small, with an RMSE of 10.64 m^3, MAE of 6.72 m^3, and MAPE of 6.76%. The coefficient of determination (R^2) was 0.948, with the fitted regression line closely aligning with the 1:1 reference line (Fig. 13). These results indicate that SlashScan provides volume estimates with sufficiently high accuracy for practical field applications, considering the inherent variability of pile size and shape under operational forestry

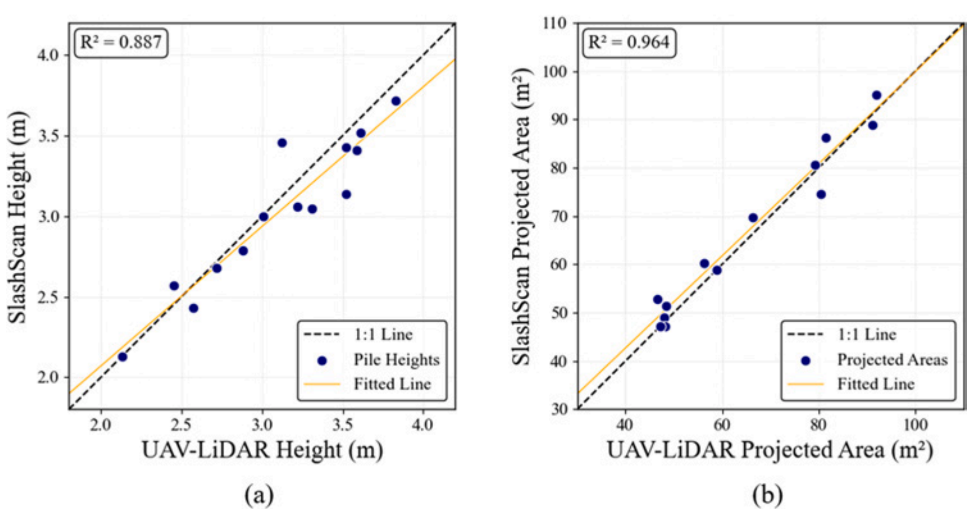

Fig. 10. Agreement between SlashScan and UAV-LiDAR for component geometric metrics. (a) Pile maximum height and (b) 2D projected area. The dashed black line represents the 1:1 reference relationship, and the orange line shows the fitted linear regression. The coefficient of determination (R^2) is shown in the upper-left corner.

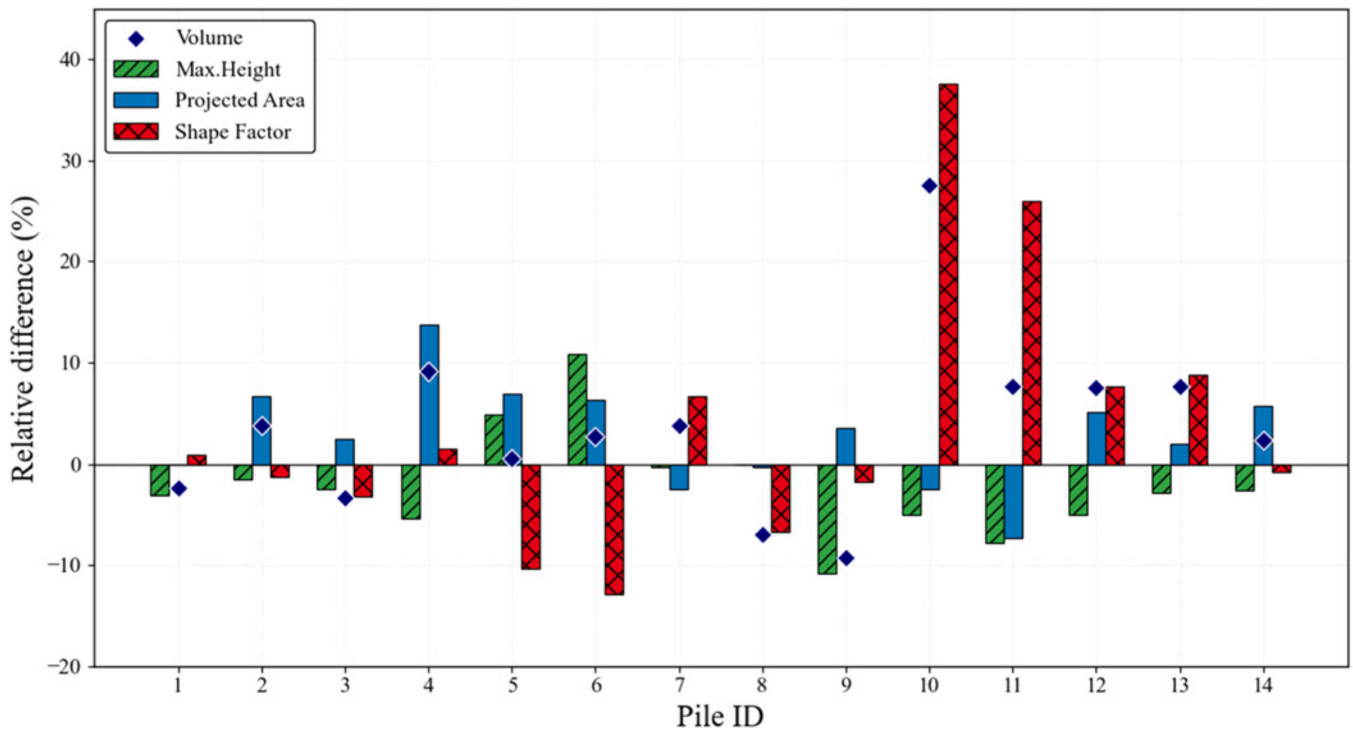

Fig. 11. Decomposition of relative volume differences into contributions from height (green, hatched), projected area (blue, solid), and shape factor (red, cross-hatched) for each pile. The shape factor $k = V / (H \times A)$ represents the fullness of the 3D pile profile relative to the bounding prism defined by pile maximum height (H) and 2D projected area (A). Diamond markers indicate the actual relative volume difference. All values are expressed as percentages relative to the corresponding UAV-LiDAR estimate.

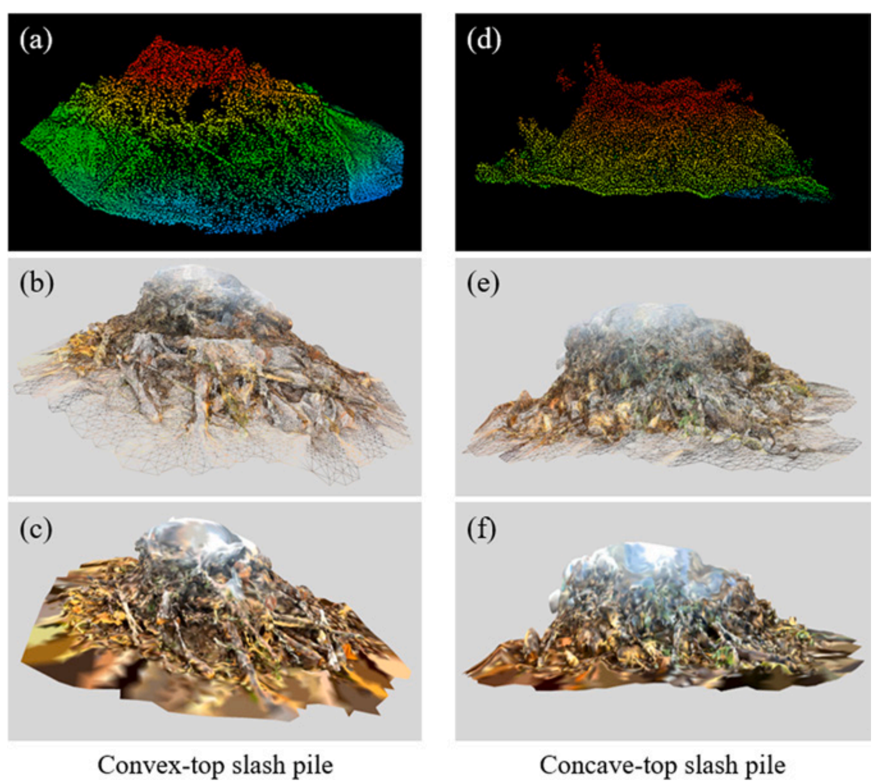

Fig. 12. Comparison of convex- and concave-top slash piles acquired from UAV-LiDAR and reconstructed by the SlashScan. (a–c) show a slash pile with a convex top (Pile ID 1 in Table 1); (d–f) Slash pile with a concave top (Pile ID 10 in Table 1). (a, d) Point-cloud representations color-coded by elevation. (b, e) Corresponding wireframe mesh showing structural surface continuity. (c, f) Final 3D models generated through PSR.

conditions.

The largest deviation occurred for Pile 10, which exhibited a

Table 2
Results of a paired *t*-test comparing the volume estimates from UAV-LiDAR and SlashScan.

T-test Results	
Statistic	Value
Degrees of freedom	13
p-value	0.134
t-statistic	1.60
95% CI Lower	-1.52
95% CI Upper	10.14

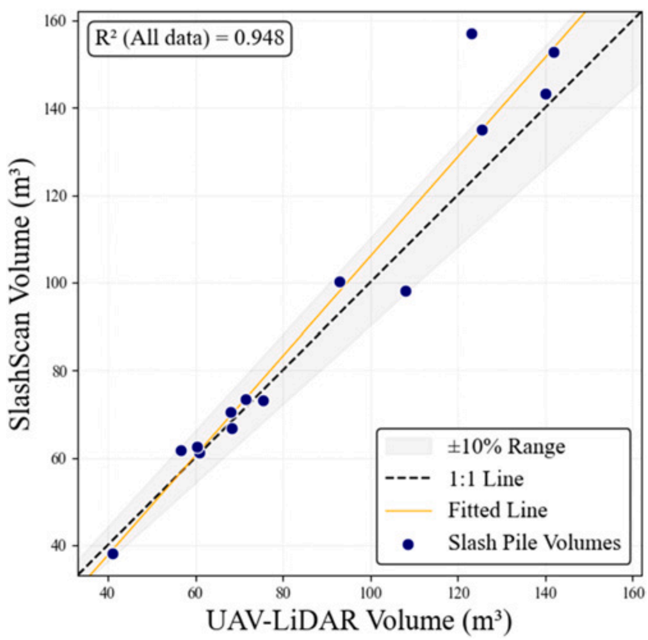

Fig. 13. Comparison of slash pile volumes estimated by SlashScan and UAV-LiDAR. The dashed black line represents the 1:1 reference relationship, and the shaded gray area indicates the ±10% agreement range. The orange line shows the fitted regression using all data. Blue dots represent individual slash pile volume measurements. The coefficients of determination (R^2) is shown in the upper-left corner.

percentage error of 27.6% attributable to upper-surface interpolation bias (see Section 3.2.2). Even with this case included in the analysis, the overall agreement between the two methods remained strong, as evidenced by the fitted regression line closely aligning with the 1:1 reference line in Fig. 13.

3.3. Research contributions, limitations, and practical implications

3.3.1. Propagation of geometric and reconstruction errors into volume discrepancy

A key contribution of this study is the explicit separation of volume discrepancy into the contributions of pile maximum height, 2D projected area, and shape factor. Because volume can be expressed as $V = H \times A \times k$, the relative volume difference between SlashScan and UAV-LiDAR can be approximated by the sum of the relative differences in these three terms. This decomposition clarifies that volume error did not arise from a single source. Instead, it emerged through the interaction of sensor-level discrepancies in pile maximum height, operator-level variability in 2D projected area delineation, and reconstruction-level discrepancies in shape factor.

The component metrics showed relatively small error levels, with MAPE values of 4.5% for pile maximum height and 4.7% for 2D projected area. For pile maximum height, SlashScan showed a consistent negative bias attributable to the limited upward viewing angle of the ground-based sensor. For 2D projected area, the small positive mean difference (2.4%) reflects variability in manual polygon delineation rather than a systematic sensor-level effect; because the operator draws the pile boundary on both platforms, individual pile-wise differences varied in both direction and magnitude. In practice, these two components tended to offset one another, so their combined contribution to final volume discrepancy was often modest. In contrast, the largest volume discrepancies were associated with deviations in shape factor, indicating that the dominant source of error was not basic geometric measurement itself but reconstruction of the 3D surface profile.

This distinction is important because global accuracy statistics such as RMSE, MAE, or MAPE describe the magnitude of the final volume error but do not reveal how that error was generated. In the present study, the shape factor analysis showed that the largest error cases arose when upper-surface occlusion forced the PSR-NBC workflow to interpolate unseen regions, particularly for tall piles with non-convex upper morphology. Thus, the results indicate that geometric measurement errors and reconstruction errors should not be treated as equivalent. For SlashScan, the former were generally small and predictable, whereas the latter were more condition-dependent and had a stronger influence on outlier cases.

3.3.2. Comparison with prior studies

The present results position SlashScan between conventional field approximations and more specialized LiDAR workflows. Geometric and manual methods have been shown to substantial estimation errors for irregular piles (Long and Boston, 2014; Zvěřina et al., 2025), while LiDAR-based approaches consistently improve estimation accuracy (Trofymow et al., 2014). The MAPE of 6.76% observed here confirms that reconstructing the actual pile form with mobile LiDAR can substantially reduce the bias associated with idealized geometric assumptions. At the same time, SlashScan is not intended as a replacement for UAV-LiDAR or TLS in all situations. Casey (2015) showed that lightweight terrestrial LiDAR could achieve strong agreement with conventional reference measurements, and the present results are consistent with that general level of performance. However, SlashScan differs in that acquisition, reconstruction, and volume computation are integrated into a consumer-grade mobile platform and completed on-device in approximately 30 s per pile, offering advantages in portability and deployment speed that are important for operational forestry.

The study also extends the scope of iOS/mobile LiDAR applications in forestry. Previous work has demonstrated the utility of consumer-grade LiDAR for forest inventory variables such as stem diameter and tree position (Gollob et al., 2021; Oikawa et al., 2025; Tatsumi et al., 2023), but those studies addressed more regular measurement targets. Slash piles are structurally more challenging because they are irregular, porous, and often contain concave or occluded upper surfaces. The present study therefore contributes not only a new application but also a clearer understanding of where error arises when mobile LiDAR is applied to this more difficult target.

3.3.3. Limitations and measurement uncertainty

Several limitations should be recognized when interpreting these results. First, measurement uncertainty arises at the sensor level. The iOS LiDAR sensor has a limited effective sensing range, and depth quality decreases as distance increases. This constraint is especially important for large piles because the upper surface may fall outside the most reliable sensing range, increasing the likelihood of incomplete sampling.

Second, uncertainty arises at the reconstruction level. The PSR-NBC framework is effective for producing continuous watertight meshes, but in regions with sparse or missing observations it must infer the surface shape from surrounding geometry. As shown by Pile 10, this can introduce a convexity bias when the true upper surface is concave or deeply occluded. The 2 cm subsampling interval also represents a tradeoff between computational efficiency and local surface detail. Although appropriate for near-real-time operation, it may smooth fine structural irregularities that would otherwise influence the reconstructed mesh.

Third, uncertainty arises at the operator level. SlashScan requires the user to circle the pile, maintain sufficient coverage, and define the cropping polygon manually. Variability in scanning distance, speed, viewing angle, and boundary delineation can affect both point-cloud completeness and the final volume estimate. In addition, the ground reference is derived from the mean coordinates of the selected polygon, which may be less accurate on uneven or sloped terrain than a more explicit local ground model. Inter-operator repeatability was not evaluated in this study and remains an important topic for future validation.

Fourth, the reference framework also imposes a limitation. UAV-LiDAR was used as the reference because direct ground-truth volume measurement for irregular slash piles is difficult under operational conditions. This is reasonable and consistent with prior literature, but UAV-LiDAR is still a reference method rather than true physical volume. Finally, the validation dataset comprised only 14 piles within a single study area. Although the range of observed pile sizes was meaningful, this sample does not capture the full diversity of pile structure, species mix, terrain, and operational conditions likely to be encountered elsewhere.

3.3.4. *Practical implications and future directions*

Despite these limitations, the results suggest that SlashScan has clear practical value for operational forestry. The system provides near-real-time, in-field volume estimates without UAV flight planning, external processing software, or specialized technical expertise. This makes it well suited for rapid decisions related to slash treatment, pile burning, and biomass recovery planning. The results also suggest a practical field interpretation rule. For piles with relatively convex upper surfaces and heights near or below the operator's eye level, SlashScan can be expected to provide robust estimates with small proportional error. For taller piles or piles likely to contain concave upper surfaces, caution is warranted because reconstruction bias may become the dominant source of error. In such cases, improved acquisition strategies, such as elevated scanning perspectives or extension-mounted devices, may reduce upper-surface occlusion and improve reliability. Taken together, these findings indicate that SlashScan can provide sufficiently reliable volume estimates under well-defined field conditions, which supports its use not only for immediate operational decisions but also as a foundation for further quantitative applications. Among these, pile mass would be a more direct metric for operational assessment, but extending validated volume estimates to mass prediction will require additional calibration using species-specific bulk density and moisture content. Such integration could support more quantitative evaluation of both fire hazard and biomass value. The present study contributes to this direction by providing and validating the volumetric foundation for those future applications.

4. Conclusion

This study developed and validated SlashScan, an iOS-based mobile application for real-time slash pile volume estimation and mapping. SlashScan integrates LiDAR-based SLAM, watertight mesh reconstruction, and on-device volumetric computation within a single mobile workflow, enabling field-based volume estimation in approximately 30 s per pile. When evaluated against a UAV-LiDAR reference across 14 slash piles, SlashScan showed strong overall agreement, with $R^2 = 0.948$, RMSE $= 10.64$ m^3, MAE $= 6.72$ m^3, and MAPE $= 6.76\%$. The paired *t*-test indicated no statistically significant difference in mean volume between the two methods at $\alpha = 0.05$. Validation of intermediate geometric quantities showed that SlashScan estimated pile maximum height and 2D projected area with relatively small error, and the shape factor decomposition demonstrated that the largest volume discrepancies arose primarily from reconstruction of the upper pile surface rather than from systematic error in the component metrics themselves. In other words, the principal limitation of the mobile workflow was not basic geometric measurement, but interpolation of incompletely observed pile morphology in tall or non-convex piles. Overall, the results indicate that SlashScan provides a practical and substantially lower-cost alternative for operational slash pile inventory where rapid field deployment and immediate results are important. Its main strengths are mobility, speed, and integration of acquisition and analysis within a single device. Its main limitations are height-dependent upper-surface occlusion, reconstruction bias in concave or poorly observed regions, operator-dependent boundary delineation, and the still-limited scope of validation. Future research should expand validation across more diverse pile conditions, evaluate repeatability across operators, improve acquisition guidance and boundary detection, and link volume estimates to biomass mass and value for end-use applications.

CRediT authorship contribution statement

Heesung Woo: Writing – review & editing, Validation, Supervision, Resources, Project administration, Methodology. **Woodam Chung:** Writing – review & editing, Supervision, Resources, Project administration, Funding acquisition. **Taejin Kim:** Writing – review & editing, Supervision. **Nathaniel Anderson:** Writing – review & editing, Resources, Project administration, Funding acquisition. **Heechan Jeong:** Writing – review & editing, Writing – original draft, Visualization, Validation, Software, Investigation, Data curation.

Declaration of Competing Interest

The authors declare that they have no known competing financial interests or personal relationships that could have appeared to influence the work reported in this paper.

Acknowledgements

This work was supported by the USDA Forest Service Rocky Mountain Research Station (Agreement No.: 22-JV-11221636-083) and Korea Forest Service through the Korea Forestry Promotion Institute (Project No.: RS-2025-2544472). The authors acknowledge Starker Forests Inc. for providing access to study sites and field support.

Data availability

Data will be made available on request.

References

Barker, J., Voorhis, J., Crotty, S.M., 2025. Assessing costs and constraints of forest residue disposal by pile burning. Front. For. Glob. Change 7, 1496190.

Bartmiński, P., Siłuch, M., Kociuba, W., 2023. The effectiveness of a UAV-based LIDAR survey to develop digital terrain models and topographic texture analyses. Sensors 23 (14), 6415.

Bojarski, W., Czekała, W., Nowak, M., Dach, J., 2023. Production of compost from logging residues. Bioresour. Technol. 376, 128878.

Brunton, A., Wuhrer, S., Shu, C., Bose, P., & Demaine, E.D. (2009). Filling holes in triangular meshes by curve unfolding. 2009 IEEE International Conference on Shape Modeling and Applications,

Casey, J.M. (2015). *Using Logging Residues as Biofuel Feedstocks in the Pacific Northwest: Estimating Slash Pile Volumes with Low-cost, Lightweight Terrestrial LiDAR*. University of Idaho.

Castel, C., D'Hoedt, M., Bonaventure, O., Jodogne, S., 2022. Automated forest inventory using the iPad Pro LiDAR scanner.

Dandois, J.P., Ellis, E.C., 2013. High spatial resolution three-dimensional mapping of vegetation spectral dynamics using computer vision. Remote Sens. Environ. 136, 259–276.

Gollob, C., Ritter, T., Kraßnitzer, R., Tockner, A., Nothdurft, A., 2021. Measurement of forest inventory parameters with Apple iPad pro and integrated LiDAR technology. Remote Sens. 13 (16), 3129.

Gotou, J. i, Nishimura, T., 2002. Pile movement and nutrient distribution in the soil around slash piles produced during whole-tree logging by a yarder and a processor. J. For. Res. 7 (4), 179–184.

Grotta, A. (2019). Don't want to burn? Other options for treating slash after a timber harvest. In O. S. University (Ed.).

Guenther, M., Heenkenda, M.K., Morris, D., Leblon, B., 2024. Tree diameter at breast height (DBH) estimation using an iPad Pro LiDAR scanner: a case study in Boreal forests, Ontario, Canada. Forests 15 (1), 214.

Han, H., Chung, W., Wells, L., Anderson, N., 2018. Optimizing biomass feedstock logistics for forest residue processing and transportation on a tree-shaped road network. Forests 9 (3), 121.

Han, S.-K., Murphy, G., 2011. Trucking productivity and costing model for transportation of recovered wood waste in Oregon. For. Prod. J. 61 (7), 552–560.

Hardy, C.C., 1996. Guidelines for estimating volume, biomass, and smoke production for piled slash, 364. US Department of Agriculture, Forest Service, Pacific Northwest Research Station.

Iglhaut, J., Cabo, C., Puliti, S., Piermattei, L., O'Connor, J., Rosette, J., 2019. Structure from motion photogrammetry in forestry: a review. Current Forestry Reports 5 (3), 155–168.

Kazhdan, M., Hoppe, H., 2013. Screened poisson surface reconstruction. ACM Trans. Graph. (ToG) 32 (3), 1–13.

Kazhdan, M., Bolitho, M., Hoppe, H., 2006. Poisson surface reconstruction. Proceedings of the fourth Eurographics symposium on Geometry processing.

Knyaz, V., Maksimov, A., 2014. Photogrammetric technique for timber stack volume contol. Int. Arch. Photogramm. Remote Sens. Spat. Inf. Sci. 40, 157–162.

Labbé, M., Michaud, F., 2011. Memory management for real-time appearance-based loop closure detection. 2011 IEEE/RSJ international conference on intelligent robots and systems.

Labbé, M., Michaud, F., 2013. Appearance-based loop closure detection for online large-scale and long-term operation. IEEE Trans. Robot. 29 (3), 734–745.

Labbé, M., Michaud, F., 2018. Long-term online multi-session graph-based SPLAM with memory management. Auton. Robots 42, 1133–1150.

Labbé, M., Michaud, F., 2019. RTAB-Map as an open-source lidar and visual simultaneous localization and mapping library for large-scale and long-term online operation. J. Field Robot. 36 (2), 416–446.

Lim, K., Treitz, P., Wulder, M., St-Onge, B., Flood, M., 2003. LiDAR remote sensing of forest structure. Prog. Phys. Geogr. 27 (1), 88–106.

Lin, J., Chen, H., Wu, R., Wang, X., Liu, X., Wang, H., Wu, Z., Cai, G., Yin, L., Lin, R., 2024. Calculating volume of pig point cloud based on improved poisson reconstruction. Animals 14 (8), 1210.

Long, J.J., Boston, K., 2014. An evaluation of alternative measurement techniques for estimating the volume of logging residues. For. Sci. 60 (1), 200–204.

McNicol, I.M., Mitchard, E.T., Aquino, C., Burt, A., Carstairs, H., Dassi, C., Modinga Dikongo, A., Disney, M.I., 2021. To what extent can UAV photogrammetry replicate UAV LiDAR to determine forest structure? A test in two contrasting tropical forests. J. Geophys. Res. Biogeosciences 126 (12) e2021JG006586.

Moe, K.T., Owari, T., Furuya, N., Hiroshima, T., Morimoto, J., 2020. Application of UAV photogrammetry with LiDAR data to facilitate the estimation of tree locations and DBH values for high-value timber species in northern Japanese mixed-wood forests. Remote Sens. 12 (17), 2865.

Mott, C.M., Hofstetter, R.W., Antoninka, A.J., 2021. Post-harvest slash burning in coniferous forests in North America: a review of ecological impacts. For. Ecol. Manag. 493, 119251.

Nurek, T., Gendek, A., Roman, K., 2019. Forest residues as a renewable source of energy: Elemental composition and physical properties. BioResources 14 (1), 6–20.

Oikawa, N., Nakagawa, Y., Owari, T., Tatsumi, S., Suzuki, S.N., 2025. Utilising LiDAR-equipped iPhone in forestry: constructing 3D models and measuring tree sizes in a planting site. Ecol. Solut. Evid. 6 (1), e12399.

Page-Dumroese, D.S., Jurgensen, M., Terry, T., 2010. Maintaining soil productivity during forest or biomass-to-energy thinning harvests in the western United States. West. J. Appl. For. 25 (1), 5–11.

Page-Dumroese, D.S., Busse, M.D., Archuleta, J.G., McAvoy, D., Roussel, E., 2017. Methods to reduce forest residue volume after timber harvesting and produce black carbon. Scientifica 2017 (1), 2745764.

Riffell, S., Verschuyl, J., Miller, D., Wigley, T.B., 2011. Biofuel harvests, coarse woody debris, and biodiversity–a meta-analysis. For. Ecol. Manag. 261 (4), 878–887.

Rusu, R.B., Cousins, S., 2011. 3d is here: Point cloud library (pcl). 2011 IEEE international conference on robotics and automation.

Son, S.W., Kim, D.W., Sung, W.G., Yu, J.J., 2020. Integrating UAV and TLS approaches for environmental management: a case study of a waste stockpile area. Remote Sens. 12 (10), 1615.

Spiers, A.I., Scholl, V.M., McGlinchy, J., Balch, J., Cattau, M.E., 2025. A review of UAS-based estimation of forest traits and characteristics in landscape ecology. Landsc. Ecol. 40 (2), 29.

Tatsumi, S., Yamaguchi, K., Furuya, N., 2023. ForestScanner: a mobile application for measuring and mapping trees with LiDAR-equipped iPhone and iPad. Methods Ecol. Evol. 14 (7), 1603–1609.

Tondo, G.R., Riley, C., Morgenthal, G., 2023. Characterization of the iPhone LiDAR-based sensing system for vibration measurement and modal analysis. Sensors 23 (18), 7832.

Trofymow, J., Coops, N., Hayhurst, D., 2014. Comparison of remote sensing and ground-based methods for determining residue burn pile wood volumes and biomass. Can. J. For. Res. 44 (3), 182–194.

Udali, A., Chung, W., Talbot, B., Grigolato, S., 2025. Managing harvesting residues: a systematic review of management treatments around the world. For. Int. J. For. Res. 98 (2), 117–135.

Vanhala, P., Repo, A., Liski, J., 2013. Forest bioenergy at the cost of carbon sequestration? Curr. Opin. Environ. Sustain. 5 (1), 41–46.

Vizzo, I., Chen, X., Chebrolu, N., Behley, J., Stachniss, C., 2021. Poisson surface reconstruction for LiDAR odometry and mapping. 2021 IEEE international conference on robotics and automation (ICRA).

Woo, H., Acuna, M., Cho, S., Park, J., 2019. Assessment techniques in forest biomass along the timber supply chain. Forests 10 (11), 1018.

Zhang, C., & Chen, T. (2001). Efficient feature extraction for 2D/3D objects in mesh representation. Proceedings 2001 International Conference on Image Processing (Cat. No. 01CH37205),

Zvěřina, L., Cibulka, M., Ulrich, R., Badal, T., Kupčák, V., 2025. Accuracy of measuring methods of pile volume of forest harvesting residues and economic impacts. Forests 16 (3), 498.